Clays and Clay Minerals, Vol. 63, No. 2, 119–131, 2015.

CLAY-MINERAL TRANSFORMATIONS AND HEAVY-METAL RELEASE IN PADDY SOILS FORMED ON SERPENTINITES IN EASTERN TAIWAN

ZENG-YEI HSEU[1,*], FRANZ ZEHETNER[2], FRANZ OTTNER[3], AND YOSHI IIZUKA[4]

[1] Department of Agricultural Chemistry, National Taiwan University, Taipei 10617, Taiwan
[2] Institute of Soil Research, University of Natural Resources and Life Sciences, A-1190 Vienna, Austria
[3] Institute of Applied Geology, University of Natural Resources and Life Sciences, A-1190 Vienna, Austria
[4] Institute of Earth Sciences, Academia Sinica, Taipei 11529, Taiwan

Abstract—Serpentinites, which contain high concentrations of Cr and Ni, weather easily into layer silicates and are therefore a possible source of metal contamination in soils. In the present study three soil profiles formed on serpentinites in a paddy field in eastern Taiwan were investigated to understand pedogenic clay-mineral transformations and to determine the relationship between the mineralogical characteristics and labile Cr and Ni in the soil. To this end, physicochemical analyses, micromorphology, X-ray diffraction, and Fourier transform infrared spectroscopy were employed. Serpentine and chlorite were the dominant minerals in the soil parent material, with smaller amounts of pyroxene, amphibole, and talc. Progressive weathering and the release of cations from the parent material resulted in the pedogenic formation of smectite, vermiculite, and interstratified chlorite-vermiculite, demonstrated by their presence in all Ap and AC horizons but their absence from the C horizons. Serpentine, pyroxene, amphibole, and talc are proposed to be transformed to low-charge smectite, while chlorite transformed to vermiculite through an interstratified chlorite-vermiculite phase. The surface soils were enriched in oxalate-extractable Fe relative to the subsoils, which was probably generated by the artificial flooding and draining of the paddy soils. The artificial flooding, which typically releases Fe, may also drive the observed partial hydroxyl interlayering of smectite and incomplete interlayer OH sheets of chlorite. Labile Cr and Ni (extracted with 0.1 N HCl) ranging from 4.7 to 26.8 mg kg^{-1} and from 56 to 365 mg kg^{-1}, respectively, increased significantly toward the surface soil, consistent with weathering. The heavy metals released may pose a threat to the environment as well as to human health by entering the food chain.

Key Words—Chlorite, Heavy Metal, Paddy Soil, Serpentine, Smectite, Vermiculite.

INTRODUCTION

Serpentinites are formed by hydrothermal metamorphism of ultramafic rocks such as peridotites and pyroxenites. During the metamorphism, the anhydrous ultramafic rocks become more hydrous and Ca content decreases, resulting in an enrichment of Mg in the serpentinites (O'Hanley, 1996). Serpentine is the name of a class of minerals of which antigorite, lizardite, and chrysotile are the most recognized members (Wicks and O'Hanley, 1988). Serpentinites also contain minor amounts of chromite, magnetite, brucite, and talc (McGahan *et al*., 2008, 2009; Morrison *et al*., 2009). Apart from spinel-group minerals with high resistance to weathering (*e.g.* chromite and magnetite) (Hseu and Iizuka, 2013), most minerals of serpentinites are relatively unstable at near-surface conditions and weather easily into other layer silicates (Rabenhorst *et al*., 1982; Dixon, 1989; Alexander, 2014). The chemical weathering of serpentinites has been studied widely for their large Cr- and Ni-ore deposits (Gaudin *et al*., 2005; Wanze *et al*., 2008; Yongue-Fouateu *et al*., 2009), but serpentinitic soils have attracted the interest of soil scientists for additional reasons. Serpentinitic soils have severe fertility limitations because of low Ca/Mg ratios (McGahan *et al*., 2008, 2009), low concentrations of P and K (Brooks, 1987; Bonifacio and Barberis, 1999), and enrichments in Cr and Ni (Hseu, 2006; Cheng *et al*., 2009; Becquer *et al*., 2010; Cheng *et al*., 2011). They further show a unique flora (Whittaker, 1954; Oze *et al*., 2008) and have unique physical properties (Alexander *et al*., 2007).

Although serpentinites cover only a small fraction of Earth's terrestrial surface area, they are abundant in ophiolite belts and widespread in regions of the Circum-Pacific margin and Mediterranean Sea (Oze *et al*., 2007). Soil-mineralogical studies have contributed significantly to the understanding of serpentinite weathering and associated environmental consequences. For instance, the release of Cr and Ni into ecosystems during serpentinite weathering suggests that serpentinite landscapes are a possible source of non-anthropogenic metal contamination (Fantoni *et al*., 2002; Oze *et al*., 2007; Morrison *et al*., 2009; Economou-Eliopoulos *et al*., 2011). Serpentine, talc, chlorite, vermiculite, smectite, and interstratified minerals have been considered as the dominant phyllosilicate minerals in serpentinitic soils under various climates (Rabenhorst *et al*., 1982; Caillaud

* E-mail address of corresponding author:
zyhseu@ntu.edu.tw
DOI: 10.1346/CCMN.2015.0630204

https://doi.org/10.1346/CCMN.2015.0630204 Published online by Cambridge University Press

et al., 2006; Hseu *et al*., 2007; Lessovaia and Polekhovsky, 2009; Garnier *et al*., 2009). The genesis of weathering products in serpentinitic soils along a moisture-regime gradient was explored by Lee *et al*. (2003) who suggested that chlorite transformed to vermiculite and interstratified chlorite-vermiculite with progressive release of Mg from the brucitic layer of the chlorite. Smectite may be inherited from parent materials (Rabenhorst *et al*., 1982), but also formed from other clay minerals in serpentinitic soils (Bonifacio *et al*., 1997; Hseu *et al*., 2007). The formation of smectite may be associated with limited cation leaching, and Mg-enriched weathering products of serpentinites may accumulate and contribute to the synthesis of smectite in poorly drained soils. In a serpentinitic soil catena of southwestern Oregon, USA, Istok and Harward (1982) found serpentine and chlorite in well drained upland soils, but serpentine, chlorite, and smectite in poorly drained soils. Bonifacio *et al*. (1997) demonstrated that serpentine could weather to low-charge vermiculite in well drained landscape positions and to smectite in poorly drained sites.

Paddy rice is an important cereal crop in global agriculture and second only to wheat in terms of the planting area of cereal crops (Kyuma, 2004). Global rice production is mainly distributed throughout Monsoon Asia with >90% of the world's rice-growing area occurring in this region (Kyuma, 2004). Serpentinitic landscapes are found commonly in Monsoon Asia, adjacent to the convergent boundary of the Eurasian Plate and the Pacific Plate. Serpentinites are generally unstable in soils (Bonifacio *et al*., 1997) and may release considerable amounts of heavy metals, notably Cr and Ni, to the environment upon weathering (Cheng *et al*., 2011). To date, only limited information is available on serpentinite weathering and associated release of heavy metals in paddy fields. An unresolved question is whether the lability of Cr and Ni in serpentinitic paddy soils is related to mineral transformations. To answer this question, we investigated paddy soil profiles formed on serpentinites in eastern Taiwan. The aims of this study were: (1) to identify the minerals and their alteration in the studied profiles, (2) to explore the transformation of clay minerals in the course of serpentinite weathering, and (3) to link the mineral weathering to the release of Cr and Ni in the soil.

MATERIALS AND METHODS

Area description and sample collection

The study area (23º42′78″ N, 121º24′46″ E) is on an alluvial plain located at the northern part of the Huadong longitudinal valley (HLV) in eastern Taiwan at an altitude of ~150 m above sea level. The HLV is a long, narrow rift stretching for ~180 km and ranging from 2 to 7 km in width, flanked by the Central Ridge to the west and the Coastal Range to the east.

The soils' parent materials in the study area contain serpentinitic alluvium of Holocene age, which originates from blocks of serpentinite that crop out in the eastern section of the Central Ridge. Three replicate pedons were selected from a paddy field, and profile pits were excavated to the depth of the C horizon. The total area of paddy fields on the alluvial plain studied is ~85,000 m^2. The distance of the paddy field studied from the upslope serpentinite sources is ~1.2 km. Paddy rice, which is generally cropped twice a year, has been produced for ~50 y in the study area. Seasonal saturation and reduction are common features in paddy rice fields in Taiwan (Hseu and Chen, 2001). During the rice-growing season, the surface soils are anoxic while the subsoils are in a more oxic state (Hseu and Chen, 1996). For a paddy soil in the HLV area, Chen (2013) reported redox potentials (Eh) from −100 to −300 mV during the rice-growing season (February−June, 2013) which increased to values between 100 and 350 mV after the soil was drained in the fallow season (July−September, 2013).

The area is characterized by high temperature and humidity. Mean annual rainfall in the study area is 1800 mm, and the mean annual air temperature is 22.5ºC (mean monthly temperatures range from 18 to 27ºC). The soil moisture regime is udic, and the soil temperature regime is hyperthermic according to US Soil Taxonomy (Soil Survey Staff, 1993).

Physical and chemical analyses

The soil samples obtained from each horizon were air-dried, ground, and passed through a 2-mm sieve for subsequent laboratory analyses. Soil particle-size distribution was determined by the pipette method (Gee and Bauder, 1986). Soil pH was measured in a mixture of soil and deionized water (1:1, w/v) using a glass electrode (McLean, 1982). Total organic carbon (OC) content was determined using the Walkley-Black wet oxidation method (Nelson and Sommers, 1982). Cation exchange capacity (CEC) and exchangeable bases (K, Na, Ca, and Mg) were determined by the ammonium acetate method (pH 7.0) (Rhoades, 1982). Total free and short-range ordered (non-crystalline) Fe (oxyhydr)oxides (Fe_d and Fe_o, respectively) were extracted with dithionite−citrate−bicarbonate (DCB) (Mehra and Jackson, 1960) and 0.2 M ammonium oxalate (pH 3.0) (McKeague and Day, 1966), respectively. Labile Cr and Ni were extracted by horizontal shaking (10-cm amplitude, 160 rpm) of 10 g of soil with 100 mL of 0.1 N HCl in polypropylene tubes for 1 h (Baker and Amacher, 1982). All extracts were filtered using Whatman No. 42 filter paper and a nitrocellulose membrane filter <0.45 μm (Millipore, Billerica, Mississippi, USA). Metal contents in all of the above solutions were determined using a flame atomic absorption spectrometer (Hitachi Z-2300, Tokyo, Japan). In addition, analysis of major and trace elements in the soil samples was conducted using wavelength-dispersive

https://doi.org/10.1346/CCMN.2015.0630204 Published online by Cambridge University Press

X-ray fluorescence (XRF). Major (Si, Al, Fe, Mg, Ca, K, Na, and Ti) and trace elements (Mn, Cr, and Ni) were measured using an XRF spectrometer (Spectro Xepos, Mahwah, New Jersey, USA), following the method of Norrish and Hutton (1969). Significant differences in basic soil characteristics and elemental contents were analyzed with Duncan's multiple range test ($p < 0.05$).

Micromorphological studies of rock and soil

For micromorphological studies, Kubiena boxes were used to collect undisturbed rock and soil blocks in the field. After air drying, vertically oriented thin sections with a thickness of 30 μm were prepared and polished by Spectrum Petrographics, Inc., Vancouver, Washington, USA. Thin sections were examined for all horizons with polarized light microscopy (Leica DM 2700 P, Wetzlar, Germany). Selected areas of uncovered thin sections were carbon-coated and further examined with a scanning electron microscope (SEM) (JEOL JSM-6360LV, Tokyo, Japan) at the Institute of Earth Sciences, Academia Sinica, Taipei, Taiwan. Back-scattered electron (BSE) images and elemental spectra by energy dispersive X-ray spectroscopy (EDX) were acquired at an accelerating voltage of 20 kV, a beam current of 20 mA, a spot size of ~1 μm, and counting times of 30 s for Si, Fe, Al, and Mg and of 20 s for the other elements. Minerals and synthetic oxides were used as standards. In addition to the approaches for undisturbed soil blocks, the surface morphology of asbestos was also examined by SEM. Fibrous materials were obtained from the surface of a fresh serpentinitic rock, freeze-dried, ground, and suspended in water. A drop of the suspension was then evaporated on a carbon-coated copper grid (300 mesh, 3.05 mm in diameter) and the prepared sample was examined by a field emission SEM (Hitachi-4700, Tokyo, Japan) in secondary electron imaging mode.

X-ray diffraction and infrared spectroscopy of rock and soil

X-ray powder diffraction (XRD) was conducted on the parent-rock material from the bottom of the soil profiles, and on clay-size fractions. The random powder XRD technique was used to determine the mineralogy of the rock. For the analysis of clay minerals with XRD and Fourier transform infrared (FTIR) spectroscopy, air-dried soil samples were pretreated with 30% H_2O_2 to remove organic matter, and then treated with the DCB method to remove iron-oxide coatings. The clay (<2 μm) fraction was separated using continuous-flow centrifugation, and cation-saturated samples were prepared using 1 M KCl and 1 M $(CH_3COO)_2Mg$. K-saturated samples were examined at room temperature and after heating to 350ºC and 550ºC, and Mg-saturated samples were examined at room temperature and after glycerol treatment. X-ray diffraction of oriented clay specimens was performed in a Rigaku D/max-2200/PC (Tokyo, Japan) with Ni-filtered CuKα radiation generated at 30 kV and 10 mA; samples were scanned from 2 to 50º2θ, at a rate of 0.2º2θ min^{-1}. Using the reciprocal mineral intensity factors summarized by Kahle *et al.* (2002), semi-quantitative determination of the clay minerals was based on the difference of reflection patterns from the K-saturated, Mg-saturated, glycolated, heated, and air-dried samples (Johns *et al.*, 1954). Additionally, selected thin sections were analyzed by means of X-ray micro diffraction using an X'Pert PRO MPD diffractometer with automatic divergence slit, Cu LFF tube (45 kV, 40 mA) and a position-sensitive X'Celerator detector (PANalytical, Almelo, the Netherlands). The X-ray beam was focused on the thin sections using a mono-capillary with a diameter of 0.5 mm. The samples were scanned at a step size of 0.017º2θ, with a measuring time of 100 s per step.

The parent-rock material and the soil clay fractions were also analyzed by FTIR spectroscopy. Samples were dried at 60ºC, ground in a steel grinder and passed through a 100-mesh sieve to form an homogeneous powder, of which 100 mg was ground in a Specamill (Specac GS06002, Swedesboro, New Jersey, USA) to a particle size of <1 μm. Powdered, dry samples (~10 mg) were ground with 1 g of dried KBr until homogeneous and pressed into pellets. Infrared (IR) absorption spectra were obtained using a Bruker Vector 22 FTIR spectrometer (Fremont, California, USA) in transmission mode from 400 to 4000 cm^{-1}, with a resolution of 4 cm^{-1} using 16 scans.

RESULTS

Parent materials

Serpentine was the major groundmass in the parent-rock material, with opaque inclusions of chromite staining the groundmass in the polarized light microscope (Figure 1a). Three polymorphs of serpentine, *i.e.* chrysotile, antigorite, and lizardite, were identified by their different textures. Veins of cross-fiber chrysotile co-exist with antigorite/lizardite in the weathered parent material (Figure 1b). In the subsoil, fragments of weathered ultramafic rocks as well as mineral particles originating from serpentinized ultramafics, *e.g.* serpentinized pyroxene (Figure 1c), were found. A small amount of strong-yellow pseudomorphs of clay and irregularly distributed brown Fe oxides on the surface of serpentine and soil structure were interpreted as transformed phases (Figure 1d).

Amphibole asbestos with needle-like shape and fiber-type chrysotile asbestos were observed using SEM (Figure 2a,b, respectively). In addition to serpentine, chlorite and chromite were found in the samples (Figure 2c,d, respectively). Analysis by EDX indicated that Cr was the predominant element in the chromite with smaller amounts of Fe, Mg, Al, and Si (Figure 2e).

Powder XRD revealed a dominance of serpentine in the parent-rock material, with prominent peaks at 0.72

https://doi.org/10.1346/CCMN.2015.0630204 Published online by Cambridge University Press

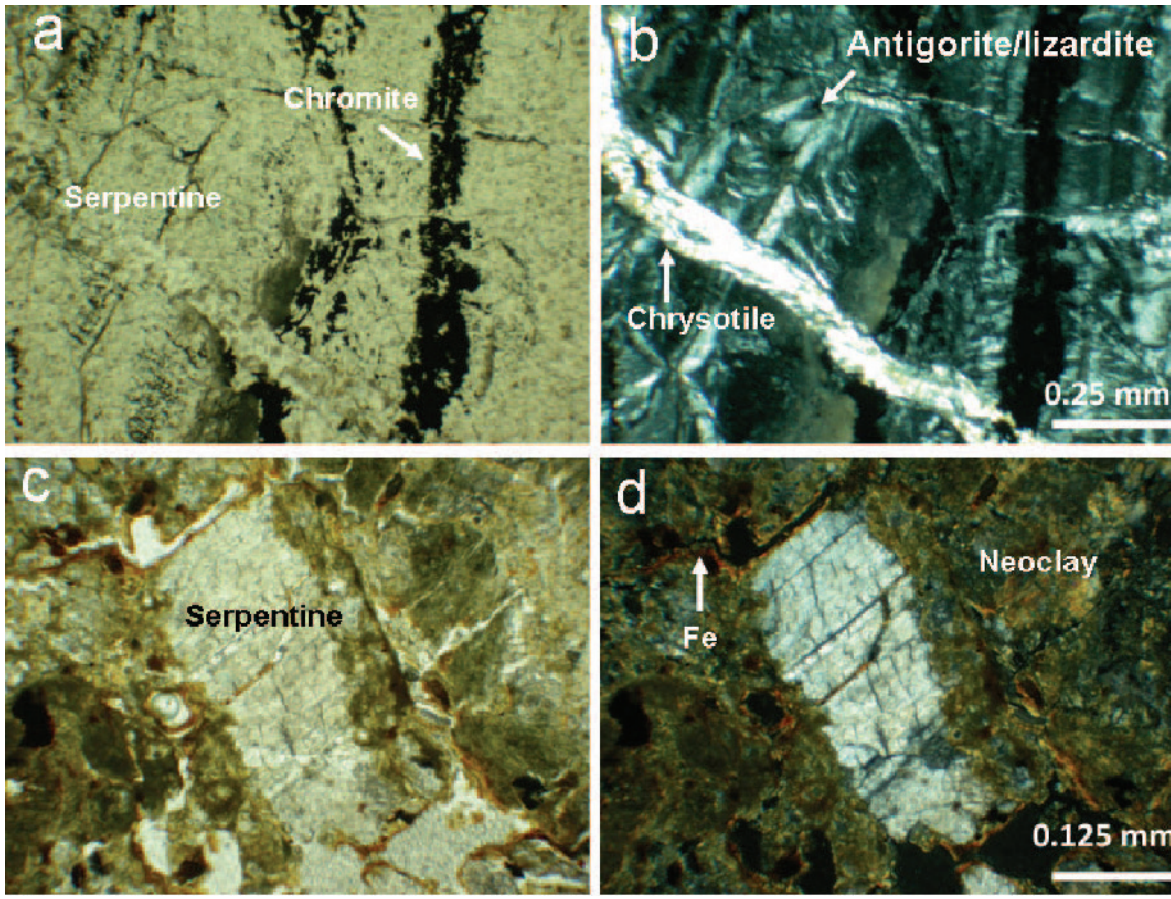

Figure 1. Photomicrographs: (a) serpentine matrix associated with opaque chromite in the parent-rock material of Pedon 1 under plane polarized light (PPL); (b) same image as (a) but under cross polarized light (XPL); (c) weathered serpentine surrounded by clay and pedogenic Fe oxides in the C horizon of Pedon 2 under PPL; (d) same image as (c) but under XPL.

and 0.36 nm (Figure 3). The XRD peaks at 1.41, 0.72, 0.48, and 0.36 nm are indicative of chlorite. In addition to serpentine and chlorite, talc (0.95, 0.46, and 0.31 nm), amphibole (0.85 nm), chromite (0.28 and 0.20 nm), mica (1.00 and 0.50 nm), quartz (0.43 and 0.34 nm), and plagioclase (0.32 nm) were also found by XRD (Figure 3). X-ray microdiffraction on a thin section from the AC horizon of Pedon 2 identified pyroxene, amphibole, chlorite, serpentine, plagioclase, muscovite, and quartz, at different spots (diameter $\approx$ 1 mm), and notably revealed areas dominated by serpentine co-existing with areas where serpentine was not detectable (Figure 4).

General soil properties

The soil textures showed small clay contents in all pedons (Table 1). The pH, which was >7.0 in all pedons, increased with soil depth. The OC content ranged between 0.9 and 1.8% and the CEC was between 5.1 and 8.6 cmol kg^{-1}. The base saturation exceeded 60%. The Fe_o/Fe_d ratio was significantly ($p < 0.05$) higher in the Ap horizons than in the subsoils, indicating a greater abundance of short-range-ordered Fe oxides near the surface. The concentrations of Cr and Ni extracted with 0.1 N HCl were clearly above the geochemical background levels in non-serpentine agricultural soils of Taiwan (~10 mg kg^{-1}, using 0.1 N HCl extraction; Jien *et al*., 2011), and increased significantly ($p < 0.05$) toward the surface in the pedons studied. The Ni concentrations were much higher than those of Cr (Table 1).

The bulk elemental compositions of the soils exhibited relatively small Si contents ranging from 208 to 264 g kg^{-1}, consistent with the Si-poor nature of ultramafic parent rocks (Table 2). Similarly, low Al contents corresponded with the geochemical characteristics of serpentinites shown in the literature (Caillaud *et al*., 2006; Hseu *et al*., 2007; Cheng *et al*., 2009). The indicator element in serpentinitic soils, Mg, was present in much larger amounts than Ca, reflecting its enrichment during metamorphism (O'Hanley, 1996). The pedons contained substantial amounts of Cr and Ni, which were greater than those found in soils from other parent materials (Bonifacio *et al*., 1997; Oze *et al*., 2008).

https://doi.org/10.1346/CCMN.2015.0630204 Published online by Cambridge University Press

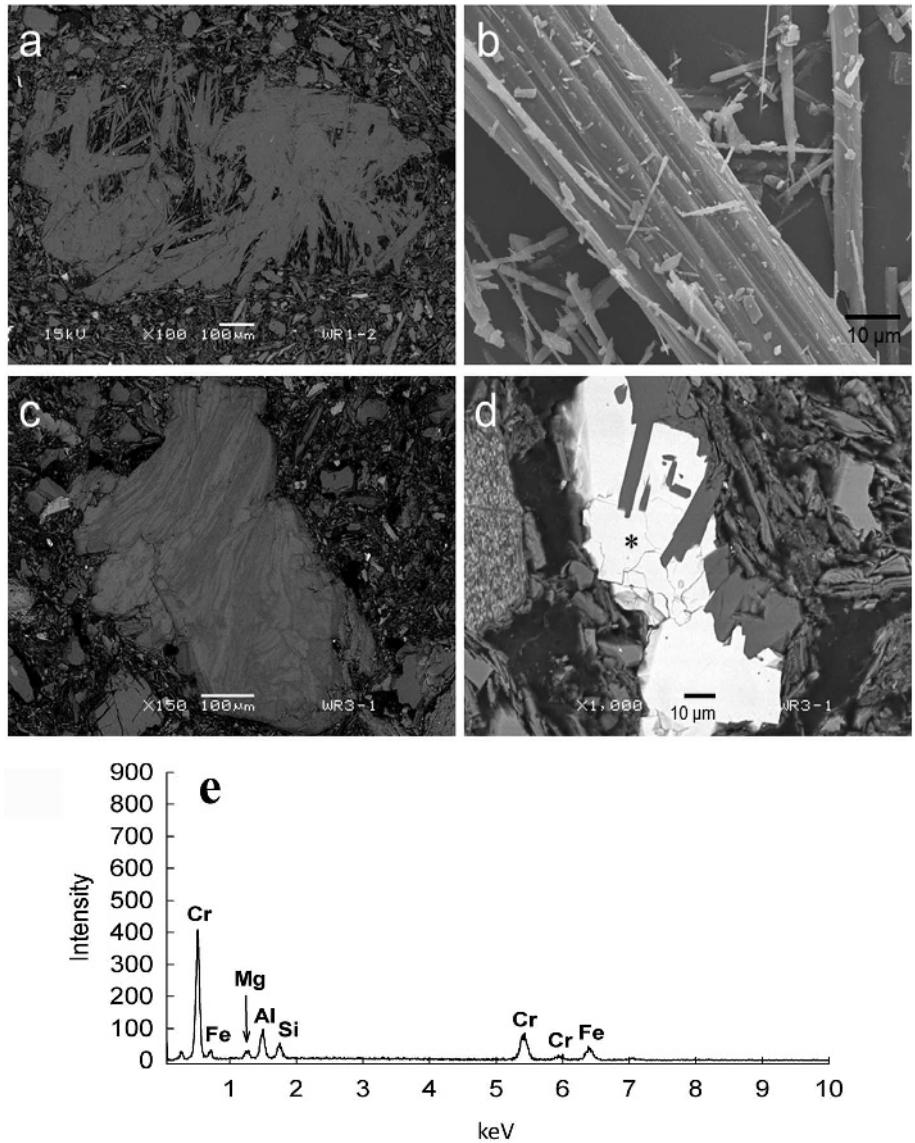

Figure 2. Back-scattered electron images of: (a) amphibole asbestos, (c) chlorite, (d) chromite, and (e) EDX spectroscopy of the spot marked with an asterisk in (d); (b) SEM secondary-electron image of chrysotile. All images from the C horizon of Pedon 3.

Clay-mineral composition

The minerals chlorite, smectite, mixed-layer chlorite-vermiculite, vermiculite, serpentine, mica, plagioclase, and chromite were identified at variable abundances in the clay fraction of the pedons studied (Table 3). The XRD patterns of the clay fraction from the Ap horizon of Pedon 3 are presented here as an example showing the clay mineralogy of the soils studied (Figure 5). Chlorite was clearly identified by the peaks at 1.41, 0.72, 0.48, and 0.36 nm, with the 0.72-nm peak being reduced when heated to 550ºC. Chlorite was present in all soils, but the amount increased with soil depth (Table 3). Smectite was identified by its 1.4 to 1.5-nm spacing after Mg saturation which expanded to ~1.82 nm after glycerol solvation and did not collapse completely to 1.0 nm after K saturation and heating to 550ºC for 2 h, suggesting partial hydroxyl interlayering of the smectite. This behavior was also observed in other studies of serpentinite-derived soils (Graham *et al*., 1990; Hseu *et al*., 2007). According to the reference d_{001} values for different treatments reported by Lee *et al*. (2003), the smectite in the studied soils was a low-charge type on the basis of the peaks at 1.82 nm with Mg saturation and glycerol solvation, 1.24 nm with K saturation at room temperature, and 1.0 nm with K saturation and heating to 550ºC (Figure 5). Vermiculite was identified by the peak at 1.41 nm at room temperature, collapsing to 1.0 nm when the K-saturated clays were heated at 350ºC. The XRD peaks at 1.41 nm in the Mg-saturated state and between 1.2 and 1.3 nm in

https://doi.org/10.1346/CCMN.2015.0630204 Published online by Cambridge University Press

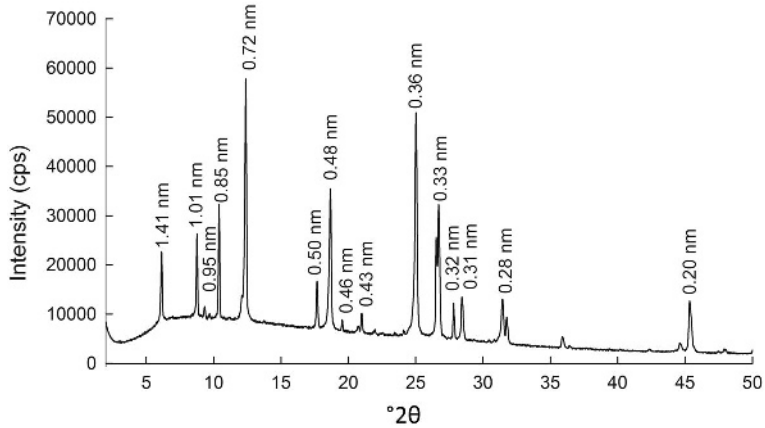

Figure 3. XRD pattern of the parent-rock material from the bottom of Pedon 1.

the K-saturated state heated at 550ºC are characteristic of randomly interstratified chlorite-vermiculite (Lee *et al*., 2003).

The FTIR spectrum of the parent-rock material exhibited characteristic IR bands in the region 3660−3770 cm^{-1} (Figure 6), which may, in part,

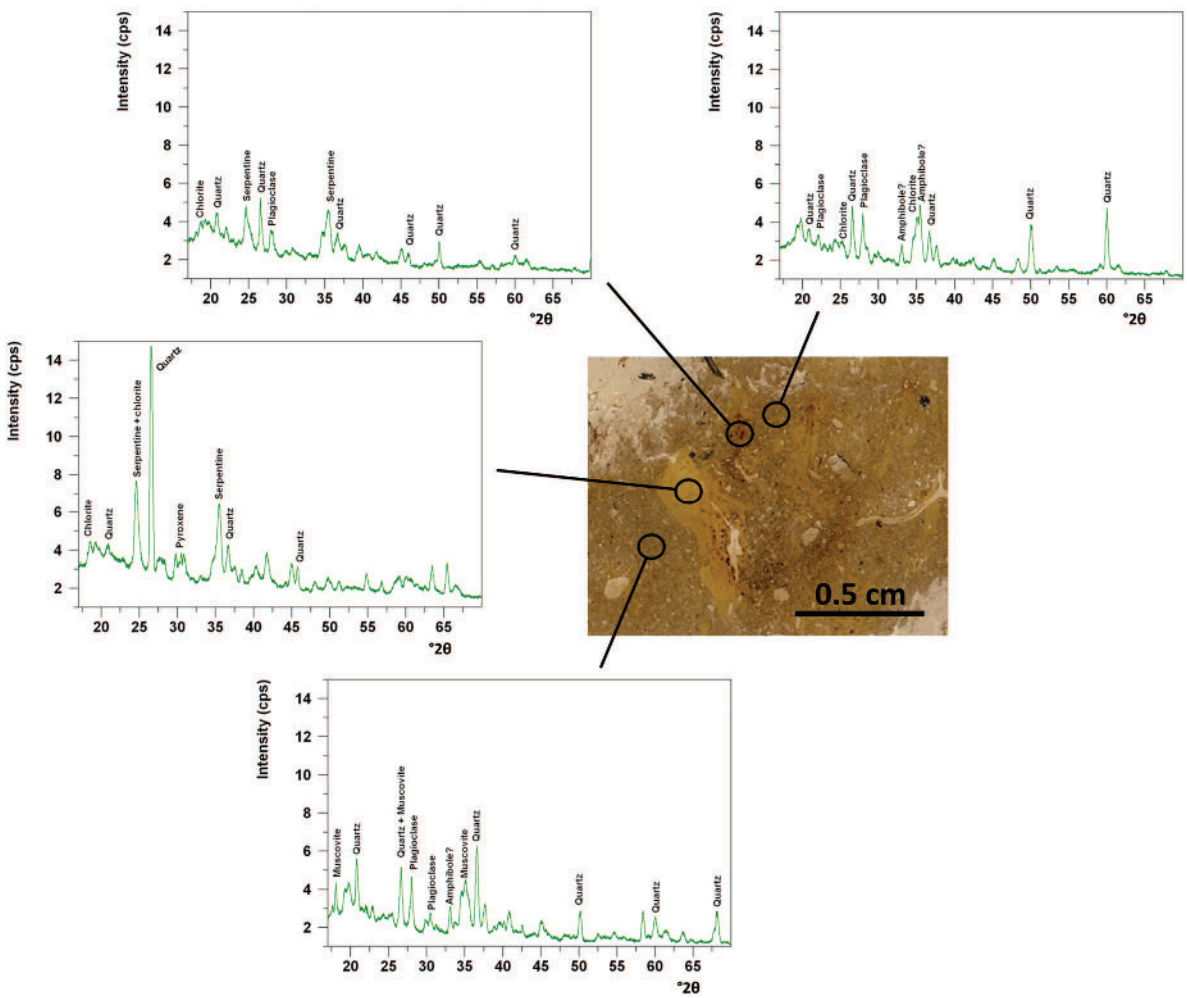

Figure 4. X-ray microdiffraction patterns of various spots (open circles, diameter ≈ 1 mm) in a thin section of the AC horizon of Pedon 2.

https://doi.org/10.1346/CCMN.2015.0630204 Published online by Cambridge University Press

https://doi.org/10.1346/CCMN.2015.0630204 Published online by Cambridge University Press

Table 1. Soil characteristics of the study pedons.

Horizon	Depth (cm)	Sand (%)	Clay (%)	pH in H_2O	OC[1] (%)	CEC[2] ($cmol_c\ kg^{-1}$)	BS[3] (%)	Fe_d[4] ($g\ kg^{-1}$)	Fe_o[5] ($g\ kg^{-1}$)	Fe_o/Fe_d	0.1 N HCl extraction Cr ($mg\ kg^{-1}$)	0.1 N HCl extraction Ni ($mg\ kg^{-1}$)
Pedon 1												
Ap	0–13	24 ± 3.5[b,6]	15 ± 2.8[a]	7.0 ± 0.1[a]	1.8 ± 0.3[a]	8.1 ± 0.5[a]	63 ± 5.3[b]	4.38 ± 0.12[b]	2.11 ± 0.08[a]	0.48 ± 0.04[a]	18.8 ± 0.47[a]	365 ± 10.4[a]
AC	13–30	29 ± 5.1[b]	11 ± 1.0[b]	7.2 ± 0.1[a]	1.3 ± 0.2[b]	5.2 ± 0.5[b]	93 ± 4.8[a]	4.84 ± 0.21[a]	1.90 ± 0.07[b]	0.39 ± 0.03[b]	12.6 ± 0.14[b]	283 ± 8.51[b]
C	>30	41 ± 3.1[a]	11 ± 1.1[b]	7.3 ± 0.2[a]	1.0 ± 0.2[b]	6.5 ± 0.7[b]	70 ± 5.6[b]	4.65 ± 0.12[a]	1.85 ± 0.10[b]	0.40 ± 0.02[b]	6.2 ± 0.2[c]	77 ± 10[c]
Pedon 2												
Ap	0–13	56 ± 3.4[a]	14 ± 2.0[a]	7.2 ± 0.1[a]	1.4 ± 0.3[a]	6.2 ± 0.1[b]	91 ± 7.3[a]	6.24 ± 0.12[c]	2.61 ± 0.11[a]	0.42 ± 0.02[a]	10.7 ± 0.23[a]	228 ± 11.3[a]
AC	13–34	55 ± 4.5[a]	14 ± 1.7[a]	7.2 ± 0.2[a]	1.1 ± 0.2[a]	5.1 ± 0.7[c]	84 ± 2.3[b]	7.13 ± 0.08[b]	1.94 ± 0.05[b]	0.27 ± 0.05[b]	6.6 ± 0.15[b]	213 ± 10.5[a]
C	>34	44 ± 4.0[b]	14 ± 2.1[a]	7.2 ± 0.2[a]	1.0 ± 0.2[a]	7.7 ± 0.4[a]	60 ± 3.5[c]	7.58 ± 0.18[a]	1.90 ± 0.09[b]	0.25 ± 0.04[b]	4.7 ± 0.1[c]	136 ± 15.1[b]
Pedon 3												
Ap	0–15	38 ± 2.5[a]	15 ± 1.2[a]	7.0 ± 0.3[a]	1.6 ± 0.2[a]	6.9 ± 0.3[b]	92 ± 6.2[a]	4.00 ± 0.12[a]	2.81 ± 0.06[a]	0.70 ± 0.05[a]	26.8 ± 0.24[a]	211 ± 10.7[a]
AC1	15–25	31 ± 2.6[b]	13 ± 1.6[ab]	7.2 ± 0.1[a]	1.8 ± 0.1[a]	8.1 ± 0.4[a]	82 ± 3.7[b]	4.81 ± 0.12[a]	2.39 ± 0.14[b]	0.50 ± 0.07[b]	25.8 ± 0.31[a]	199 ± 11.6[a]
AC2	25–40	33 ± 3.7[b]	14 ± 1.0[a]	7.3 ± 0.1[a]	1.4 ± 0.2[a]	6.2 ± 0.5[b]	96 ± 5.5[a]	4.36 ± 0.12[a]	2.27 ± 0.08[b]	0.52 ± 0.03[b]	14.1 ± 0.54[b]	112 ± 8.76[b]
C	>40	40 ± 3.0[a]	11 ± 0.1[b]	7.4 ± 0.2[a]	0.9 ± 0.1[b]	8.6 ± 0.3[a]	85 ± 1.3[b]	4.97 ± 0.12[a]	2.14 ± 0.06[b]	0.43 ± 0.03[c]	11.1 ± 0.25[b]	56 ± 7.5[c]

[1] Organic carbon
[2] Cation exchange capacity
[3] Base saturation
[4] Dithionite-extractable Fe
[5] Oxalate-extractable Fe
[6] Values followed by different letters within the same column and pedon are significantly different (Duncan's multiple range test, $p < 0.05$)

Table 2. Total concentrations of major and trace elements in the study pedons.

Horizon	Si	Al	Fe	Mg	Ca	K	Na	Ti	Mn	Cr	Ni
	(g kg^{-1})									(mg kg^{-1})	
Pedon 1											
Ap	208 ± 5.26^{b,1}	0.44 ± 0.04^{c}	13.0 ± 0.41^{b}	1.76 ± 0.15^{c}	0.55 ± 0.03^{a}	20.2 ± 2.13^{a}	4.83 ± 0.87^{a}	0.48 ± 0.34^{a}	0.78 ± 0.10^{a}	389 ± 12.1^{a}	962 ± 42.6^{b}
AC	210 ± 7.08^{b}	0.77 ± 0.06^{b}	15.8 ± 1.20^{a}	5.43 ± 0.11^{b}	0.29 ± 0.03^{b}	11.5 ± 2.14^{b}	2.13 ± 0.08^{b}	0.65 ± 0.24^{a}	0.78 ± 0.08^{a}	389 ± 10.4^{a}	965 ± 25.8^{b}
C	264 ± 11.2^{a}	1.11 ± 0.05^{a}	16.6 ± 1.52^{a}	9.47 ± 0.21^{a}	0.29 ± 0.02^{b}	10.8 ± 0.87^{b}	1.32 ± 0.12^{b}	0.75 ± 0.11^{a}	0.70 ± 0.11^{a}	348 ± 20.7^{b}	1020 ± 34.2^{a}
Pedon 2											
Ap	233 ± 12.1^{a}	1.06 ± 0.08^{b}	13.6 ± 1.71^{a}	1.79 ± 0.34^{c}	0.46 ± 0.05^{a}	16.9 ± 3.45^{a}	4.65 ± 0.43^{a}	0.35 ± 0.21^{a}	0.59 ± 0.12^{a}	342 ± 22.8^{b}	911 ± 22.3^{a}
AC	228 ± 10.4^{a}	1.27 ± 0.07^{a}	13.2 ± 0.82^{a}	2.98 ± 0.26^{b}	0.31 ± 0.04^{b}	16.7 ± 4.80^{a}	3.57 ± 0.37^{b}	0.38 ± 0.12^{a}	0.78 ± 0.09^{a}	389 ± 19.7^{a}	962 ± 50.4^{a}
C	210 ± 3.52^{b}	1.06 ± 0.04^{b}	13.7 ± 1.34^{a}	4.39 ± 0.61^{a}	0.28 ± 0.04^{b}	20.2 ± 2.34^{a}	2.85 ± 0.43^{b}	0.48 ± 0.20^{a}	0.72 ± 0.09^{a}	342 ± 31.0^{b}	944 ± 34.5^{a}
Pedon 3											
Ap	241 ± 8.64^{a}	0.64 ± 0.07^{c}	11.7 ± 1.52^{c}	1.89 ± 0.54^{c}	0.32 ± 0.03^{a}	12.1 ± 0.97^{b}	1.03 ± 0.04^{b}	0.52 ± 0.15^{a}	0.80 ± 0.08^{a}	421 ± 14.9^{a}	979 ± 20.4^{a}
AC1	228 ± 11.0^{a}	0.81 ± 0.05^{b}	15.9 ± 0.80^{b}	2.15 ± 0.58^{c}	0.31 ± 0.02^{a}	13.4 ± 1.14^{b}	1.09 ± 0.12^{b}	0.53 ± 0.14^{a}	0.81 ± 0.07^{a}	462 ± 24.6^{a}	901 ± 12.3^{b}
AC2	225 ± 7.52^{a}	0.64 ± 0.05^{c}	18.8 ± 0.81^{a}	3.79 ± 0.64^{b}	0.25 ± 0.04^{b}	18.4 ± 1.87^{a}	2.63 ± 0.45^{a}	0.46 ± 0.20^{a}	0.79 ± 0.10^{a}	389 ± 21.4^{b}	962 ± 15.7^{a}
C	223 ± 8.51^{a}	1.01 ± 0.07^{a}	17.8 ± 1.03^{a}	4.59 ± 0.42^{a}	0.25 ± 0.03^{b}	18.4 ± 2.56^{a}	3.48 ± 0.51^{a}	0.55 ± 0.08^{a}	0.68 ± 0.09^{a}	312 ± 13.5^{c}	980 ± 22.5^{a}

[1] Values followed by different letters within the same column and pedon are significantly different (Duncan's multiple range test, $p < 0.05$)

correspond to the OH-stretching vibration of talc (Bangira *et al*., 2011). Moreover, the trioctahedral minerals chlorite, talc, and serpentine, identified in the rock powder on the basis of XRD (Figure 3), show a band near 3680 cm^{-1}, which has been assigned to stretching vibrations of Mg_3OH (Farmer, 1974; Lessovaia *et al*., 2012). Furthermore, the band at 670 cm^{-1} has been ascribed to O-H libration and supports the presence of talc in the parent-rock material (Nkoumbou *et al*., 2008). The band at 467 cm^{-1} has been ascribed to an out-of-plane bending mode of Mg octahedra and assigned to serpentine (Suquet, 1989). All of the above-mentioned bands, however, were much more distinct in the parent-rock material compared to the clay fractions of the soils (cf. Figure 6). The distinct IR band at 819 cm^{-1}, which was found in the clay fractions of the soils but not in the parent-rock material (Figure 6), is a characteristic feature of Fe-rich smectites such as nontronite. The 819 cm^{-1} band may originate from OH-bending vibrations at the Fe(III)-OH site, indicating Fe in the octahedral sheet of smectite (Bangira *et al*., 2011). Hence, the presence of this band in the clay fractions of the soils and its absence from the parent-rock material seems to confirm the XRD data of decreasing smectite with soil depth (cf. Table 3).

DISCUSSION

Based on the soil morphology and basic soil properties (Table 1), the pedons studied were all classified as Lithic Udorthents according to US Soil Taxonomy (Soil Survey Staff, 2010), which formed during the Holocene and which are incipient in soil development. Nevertheless, soil-chemical parameters and clay mineralogy clearly showed progressive weathering towards the soil surface. For example, the total Mg/Ca ratio decreased substantially, *e.g.* from 32 in the C horizon to 3.2 in the Ap horizon of Pedon 1 (Table 2) based on the total analysis of elements. Such changes in the Mg/Ca ratio have been attributed to the degree of soil weathering (McGahan *et al*., 2009).

Based on the micromorphology, XRD, and FTIR analyses, abundant serpentine and chlorite were found in all pedons. In addition, pyroxene, amphibole, talc, and chromite were present in the parent-rock materials. These minerals are characteristic of serpentinites (Alexander *et al*., 2007), and their weathering releases Cr and Ni and may lead to the formation of various clay minerals (Lee *et al*., 2003; Hseu *et al*., 2007). These clay phases also generally contain some adsorbed Cr and Ni (Caillaud *et al*. 2006; Hseu *et al*., 2007; Garnier *et al*., 2009). In the present study, the dominant pedogenic minerals were smectite, vermiculite, and interstratified chlorite-vermiculite; they were present in all Ap and AC horizons but absent from the C horizons; in Pedon 3, in particular, they showed a clear increase towards the soil surface (Table 3).

https://doi.org/10.1346/CCMN.2015.0630204 Published online by Cambridge University Press

Table 3. Semi-quantitative clay-mineral composition in the study pedons[1].

Horizon	Chl	Sme	C-V	Ver	Ser	Mica	Pla	Chr
Pedon 1								
Ap	++[2]	+	+	+	+	+	+	+
AC	+++	+	+	+	++	–	+	+
C	+++	–	–	–	++	–	+	++
Pedon 2								
Ap	++	+	+	+	+	+	–	+
AC	+++	+	+	+	++	–	+	+
C	+++	–	–	–	++	–	+	+
Pedon 3								
Ap	++	+	++	++	+	+	–	+
AC1	++	+	+	+	+	–	–	+
AC2	+++	+	+	+	++	–	+	+
C	+++	–	–	–	++	–	+	++

[1] Chl: chlorite; Sme: smectite; C-V: chlorite-vermiculite mixed layers; Ver: vermiculite; Ser: serpentine; Pla: plagioclase; Chr: chromite.
[2] +++: 25–50%; ++: 10–25%; +: <10%; –: undetectable.

The parent-rock materials and soils also contained mica, plagioclase, and quartz (Figures 3 and 4, Table 3). In previous studies of ultramafic-derived soils in temperate regions, trace amounts of mica, quartz, and feldspars were reported and attributed to aeolian deposition or colluvial materials from other sources (Alexander *et al*., 2007). These minerals probably originated from mixing of the serpentinite material with other material during colluvial and alluvial transport. This is substantiated by the co-existence of areas with distinct mineralogy identified by X-ray on thin sections (Figure 4). Long-distance aeolian transport was shown by Hseu *et al.* (2007) to have supplied little quartz in the HLV area of eastern Taiwan.

A principal distinction between paddy soils and upland soils is the variations in oxidation and reduction status, which may strongly affect clay mineralogy (Kögel-Knabner *et al*., 2010). Favre *et al*. (2002) investigated the changes in structural mineral iron in a soil, containing smectite and kaolinite as the dominant clay minerals, that was cropped with paddy rice twice a year for 11 y . They found that structural smectite Fe^{2+} increased upon reduction but, nevertheless, the Fe contents of the Ap horizon were less than those in soils of uncropped neighboring land, suggesting that inundation induced weathering and eluviation of the released elements.

The parent materials of the studied soils, containing pyroxene, amphibole, talc, serpentine, and chlorite, are

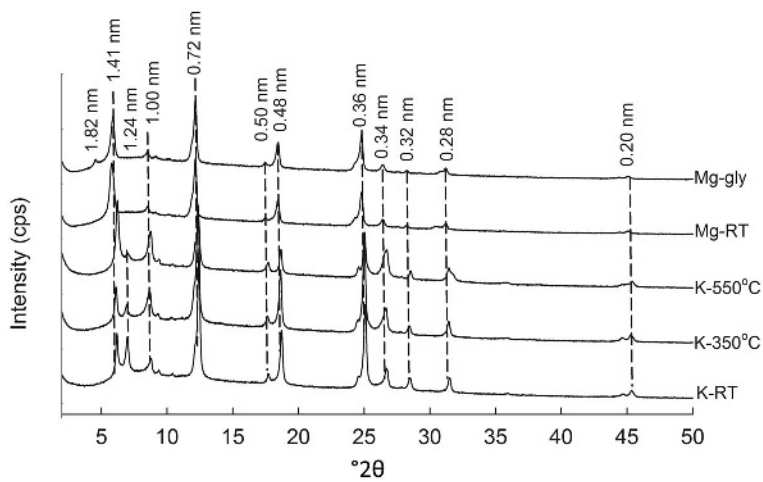

Figure 5. XRD patterns of the clay fraction from the Ap horizon of Pedon 3, with K-saturated treatments at room temperature (K-R*T*), 350ºC, and 550ºC, and with Mg-saturated treatments at room temperature (Mg-R*T*) and after glycerol solvation (Mg-Gly).

https://doi.org/10.1346/CCMN.2015.0630204 Published online by Cambridge University Press

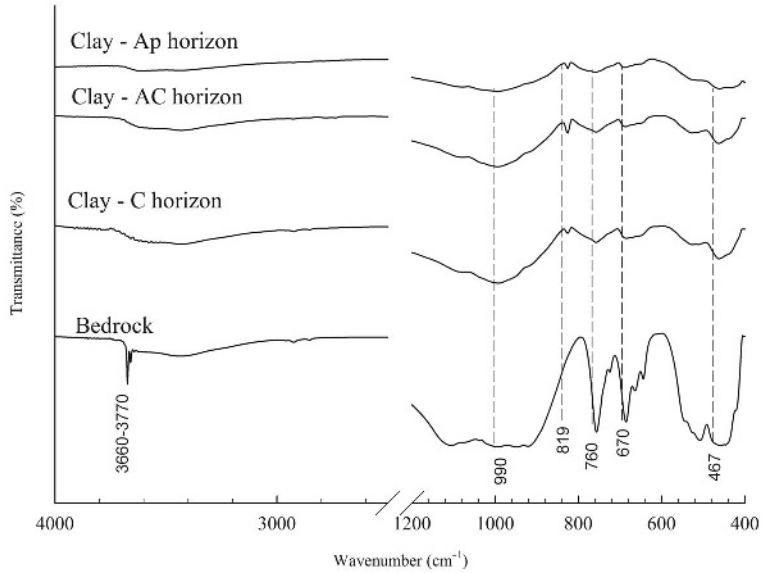

Figure 6. FTIR spectra of parent-rock material and clay fractions from the three horizons of Pedon 2.

relatively unstable in the field (Hseu *et al*., 2007; McGahan *et al*., 2008; Lessovaia *et al*., 2012), and weathered readily in these paddy soils exposed to tropical climate, with an initial loss of cations, notably Mg and Fe (Table 2), from the mineral structures (Berner and Schott, 1982). Release of these cations probably facilitated the formation of smectite (nontronite), vermiculite, and interstratified chlorite-vermiculite under conditions of limited percolation in the soils (Bonifacio *et al*., 1997; Lee *et al*., 2003).

The flooding required for paddy rice production might also make the studied soils prone to ferrolysis (Kyuma, 2004). This process could explain the relative increase in short-range-ordered Fe oxides in the Ap horizons compared to the AC or C horizons (cf. Fe_o/Fe_d; Table 1), while there was no difference in Fe_o/Fe_d between surface soil and subsoil in upland soils of a serpentinitic toposequence in eastern Taiwan (Hseu, 2006). The Fe released could also be involved in the observed partial hydroxyl interlaying of smectite and incomplete interlayer OH sheets of chlorite (Dousova *et al*., 2014). Also, the FTIR spectra suggest the formation of Fe-rich smectite (Figure 6).

Serpentine and chlorite were suggested by Lee *et al*. (2003) to have transformed into low-charge and high-charge smectites, respectively, in poorly drained soils from serpentinites in California, but only low-charge smectite was found in the present study. The removal of Fe and Mg from the interlayer OH sheets is an important step in the weathering of chlorite to vermiculite. Vermiculite further transforms to high-charge smectite through a loss of charge in the octahedral sheet as Fe^{2+} is oxidized (Bonafacio *et al*., 1997). The flooding, however, might have retarded the oxidation of Fe^{2+} to form high-charge smectite from vermiculite in this study. Based on the aforementioned findings, the following pathways are proposed for the mineral transformation in the paddy soils studied:

(1) Pyroxene, amphibole, and talc → low-charge smectite
(2) Serpentine → low-charge smectite
(3) Chlorite → interstratified chlorite-vermiculite → vermiculite

The susceptibility of serpentine minerals to weathering has been linked to enhanced availability of Cr and Ni in serpentine soils (Caillaud *et al*., 2006; Morrison *et al*., 2009; Cheng *et al*., 2011). In the present study, all pedons showed a marked enrichment of labile Cr and Ni in the surface soils relative to the subsoils (Table 1). These depth trends probably reflect the release of Cr and Ni upon weathering of the ultramafic parent material followed by their sorption (in labile form) on the surfaces of transformed clay minerals. Other, external sources of Cr and Ni probably play a minor role. No industrial activity exists in the HLV area, and strict regulation standards imposed by the Taiwanese government limit the input of heavy metals from irrigation water and compost. In Taiwan, the limits of Cr and Ni for irrigation water are 0.1 and 0.2 mg L^{-1}, respectively, and the control standards for compost are 50 and 25 mg kg^{-1}, respectively. The concentrations of Cr and Ni in the irrigation water in the vicinity of the studied paddy field were below the detection limit (<0.005 mg L^{-1}) (Chang, 2014). Little manure compost (<10 ton ha^{-1} y^{-1}) has been applied to the studied soils, contributing only trace amounts of Cr and Ni. Therefore, the main source of Cr and Ni in the studied soils appears to be the parent material rather than dust, fertilizer, or irrigation. This is in line with a number of studies that have shown high concentrations of Cr and Ni originating from parent

https://doi.org/10.1346/CCMN.2015.0630204 Published online by Cambridge University Press

materials in serpentinitic soils without human activities (Bonifacio *et al*., 1997; Hseu, 2006; Hseu *et al*., 2007; Garnier *et al*., 2009; Cheng *et al*., 2011).

Compared to serpentine and chlorite, chromite, which is a primary Cr-bearing mineral in serpentinitic soils, is much more resistant to weathering (Hseu and Iizuka, 2013). This probably explains why the amount of extractable Cr was much smaller than the extractable Ni in this study. While the observed release of Cr and Ni may pose a threat to the environment and to human health, the present authors also found fibrous minerals including amphibole and chrysotile asbestos in the studied paddy soils (Figure 2), which are known human carcinogens (International Agency for Research on Cancer, 2012) and may cause disease if inhaled by humans (Camargo *et al*., 2011).

CONCLUSIONS

The studied paddy soils are incipient in their development. Nevertheless, clear indications of chemical weathering and mineral transformations toward the soil surface were found. Fe and Mg were released from the ultramafic parent material, and the minerals of the parent material were transformed to secondary minerals, notably low-charge smectite, vermiculite, and mixed-layer chlorite-vermiculite. These findings support the low stability of serpentinites reported in previous studies. In the present study, the observed weathering of the serpentinitic parent material resulted in a marked release of labile Cr and Ni toward the soil surface. This shows that even in slightly developed serpentinitic soils (Entisols), weathering under paddy-rice production (*i.e.* alternating redox conditions) and tropical climate can lead to a significant release of heavy metals from the parent material. These could pose a threat to the environment and to human health.

ACKNOWLEDGMENTS

The authors thank the Ministry of Science and Technology of the Republic of China, Taiwan for supporting this research financially under Contracts No. NSC 99-2313-B-020-010-MY3 and NSC 102-2313-B020-009-MY3.

REFERENCES

Alexander, E.B. (2014) Arid to humid serpentine soils, mineralogy, and vegetation across the Klamath Mountains, USA. *Catena*, **116**, 114–122.

Alexander, E.B., Coleman, R.G., Keeler-Wolf, T., and Harrison, S. (2007) Serpentine soil distributions and environmental influences. Pp. 55–78 in: *Serpentine Geoecology of Western North America* (E.B. Alexander, R.G. Coleman, T. Keeler-Wolf, and S. Harrison, editors). Oxford University Press, New York.

Baker, D.E. and Amacher, M.C. (1982) Nickel, copper, zinc, and cadmium, Pp. 323–336 in: *Methods of Soil Analysis, Part 2, Chemical and Microbiological Properties*, 2nd edition (A.L. Page, R.H. Miller, and D.R. Keeney, editors). Agronomy Monograph No. **9**, Agronomy Society of America and Soil Science Society of America, Madison, Wisconsin, USA.

Bangira, C., Deng, Y., Loeppert, R.H., Hallmark, C.T., and Stucki, J.W. (2011) Soil mineral composition in constrasting climatic regions of the Great dyke, Zimbabwe. *Soil Science Society of America Journal*, **75**, 2367–2378.

Becquer, T., Quantin, C., and Boudot, J.B (2010) Toxic levels of metals in Ferralsols under natural vegetation and crops in New Caledonia. *European Journal of Soil Science*, **61**, 994–1004.

Berner, R.A. and Schott, J. (1982) Mechanism of pyroxene and amphibole weathering: II. Observations of soil grains. *American Journal of Science*, **282**, 1214–1231.

Bonifacio, E. and Barberis, E. (1999) Phosphorus dynamics during pedogenesis on serpentinite. *Soil Science*, **164**, 960–968.

Bonifacio, E., Zanini, E., Boero, V., and Franchini-Angela, M. (1997) Pedogenesis in a soil catena on serpentinite in northwestern Italy. *Geoderma*, **75**, 33–51.

Brooks, R.R. (1987) *Serpentine and its Vegetation: a Multidisciplinary Approach*. Croom Helm, London.

Caillaud, J., Proust, D., and Righi, D. (2006) Weathering sequences of rock-forming minerals in a serpentinite: influence of microsystems on clay mineralogy. *Clays and Clay Minerals*, **54**, 87–100.

Camargo, M., Stayner, L., Straif, K., Reina, M., Al-Alem, U., Demers, P., and Landrigan, P. (2011) Occupational exposure to asbestos and ovarian cancer. *Environmental Health Perspectives*, **119**, 1211–1217.

Chang, Y.C. (2014) The investigation of extractable Cr and Ni concentrations and soil properties for serpentinitic soils. Master Thesis, Department of Environmental Science and Engineering, National Pingtung University of Science and Technology, Pingtung, Taiwan, 62 pp. (in Chinese with English abstract).

Chen, Y. (2013) Heavy metals uptake of paddy rice on serpentine soils with different fertilizer treatments. Master Thesis, Department of Environmental Science and Engineering, National Pingtung University of Science and Technology, Pingtung, Taiwan, 70 pp. (in Chinese with English abstract).

Cheng, C.H., Jien, S.H., Tsai, H., Chang, Y.H., Chen, Y.C., and Hseu, Z.Y. (2009) Geochemical element differentiation in serpentine soils from the ophiolite complexes, eastern Taiwan. *Soil Science*, **174**, 283–291.

Cheng, C.H., Jien, S.H., Iizuka, Y., Tsai, H., Chang, Y.H., and Hseu, Z.Y. (2011) Pedogenic chromium and nickel partitioning in serpentine soils along a toposequence. *Soil Science Society of America Journal*, **75**, 659–668.

Dixon, J.B. (1989) Kaolin and serpentine group minerals. Pp. 467–526 in: *Minerals in Soil Environments*, 2nd edition (J.B. Dixon and S.B. Weed, editors). Soil Science Society of America Book Series No. **1**, Soil Science Society of America, Madison, Wisconsin, USA.

Dousova, B., Fuitova, L., Kolousek, D., Lhotka, M., Grygar, T.M., and Spurna, P. (2014) Stability of iron in clays under different leaching conditions. *Clays and Clay Minerals*, **62**, 145–152.

Economou-Eliopoulos, M., Megremi, I., and Vasilatos, C. (2011) Factors controlling the heterogeneous distribution of Cr(VI) in soil, plants and groundwater: Evidence from the Assopos basin, Greece. *Chemie der Erde*, **71**, 39–52.

Fantoni, D., Brozzo, G., Canepa, M., Cipolli, F., Marini, L., Ottonello, G., and Zuccolini, M.V. (2002) Natural hexavalent chromium in groundwaters interacting with ophiolitic rocks. *Environmental Geology*, **42**, 871–882.

Farmer, V.C. (1974) The layer silicates. Pp. 331–364 in: *The Infrared Spectra of Minerals* (V.C. Famer editor).

https://doi.org/10.1346/CCMN.2015.0630204 Published online by Cambridge University Press

Monograph No. **4**, Mineralogical Society, London.
Favre, F., Tessier, D., Abdelmoula, M., Génin, J.M., Gates, W.P., and Boivin, P. (2002) Iron reduction and changes in cation exchange capacity in intermittently waterlogged soil. *European Journal of Soil Science*, **53**, 175–183.
Garnier, J., Quantin, C., Guimarães, E., Garg, V.K., Martins, E.S., and Becquer, T. (2009) Understanding the genesis of ultramafic soils and catena dynamics. *Geoderma*, **151**, 204–214.
Gaudin, A., Decarreau, A., Noack, Y., and Graby, O. (2005) Clay mineralogy of the nickel laterite ore developed from serpentinised peridotites at Murrin Murrin, Western Australia. *Australian Journal of Earth Science*, **52**, 231–241.
Gee, G.W. and Bauder, J.W. (1986) Particle-size analysis. Pp. 383–411 in: *Methods of Soil Analysis*, Part 1, 2nd edition (A. Klute, editor). Agronomy Monograph No. **9**. American Society of Agronomy and Soil Science Society of America, Madison, Wisconsin, USA.
Graham, R.C., Diallo, M.M., and Lund, L.J. (1990) Soils and mineral weathering on phyllite colluvium and serpentinite in northwestern California. *Soil Science Society of America Journal*, **54**, 1682–1690.
Hseu, Z.Y. (2006) Concentration and distribution of chromium and nickel fractions along a serpentinitic toposequence. *Soil Science*, **171**, 341–353.
Hseu, Z.Y. and Chen, Z.S. (1996) Saturation, reduction, and redox morphology of seasonally flooded Alfisols in Taiwan. *Soil Science Society of America Journal*, **60**, 941–949.
Hseu, Z.Y. and Chen, Z.S. (2001) Quantifying soil hydromorphology of a rice-growing Ultisol toposequence in Taiwan. *Soil Science Society of America Journal*, **65**, 270–278.
Hseu, Z.Y. and Iizuka, Y. (2013) Pedogeochemical characteristics of chromite in a paddy soil derived from serpentinites. *Geoderma*, **202–203**, 126–133.
Hseu, Z.Y., Tsai, H., Hsi, H.C., and Chen, Y.C. (2007) Weathering sequences of clay minerals in soils along a serpentinitic toposequence. *Clays and Clay Minerals*, **55**, 389–401.
International Agency for Research on Cancer (2012) Asbestos. Pp. 219–294 in: *A Review of Human Carcinogens*. IARC Monograph on the Evaluation of Carcinogenic Risks to Humans **100C**. WHO Press, Lyon, France.
Istok, J.D. and Harward, M.E. (1982) Influence of soil moisture on smectite formation in soils derived from serpentinite. *Soil Science Society of America Journal*, **46**, 1106–1108.
Jien, S.H., Tsai, C.C., Hseu, Z.Y., and Chen, Z.S. (2011) Baseline concentrations of toxic elements in metropolitan park soils of Taiwan. *Terrestrial and Aquatic Environmental Toxicology*, **5**, 1–7.
Johns, W.D., Grim, R.E., and Bradley, W.F. (1954) Quantitative estimations of clay minerals by diffraction methods. *Journal of Sedimentary Petrology*, **24**, 242–251.
Kahle, M., Kleber, M., and Jahn, R. (2002) Review of XRD-based quantitative analyses of clay minerals in soils: the suitability of mineral intensity factors. *Geoderma*, **109**, 191–205.
Kögel-Knabner, I., Amelung, W., Cao, Z., Fiedler, S., Frenzel, P., Jahn, R., Kalbitz, K., Kölbl, A., and Schloter, M. (2010) Biogeochemistry of paddy soils. *Geoderma*, **157**, 1–14.
Kyuma, K. (2004) *Paddy Soil Science*. Kyoto University Press, Kyoto, Japan, 280 pp.
Lee, B.D., Sears, S.K., Graham, R.C., Amrhein, C., and Vali, H. (2003) Secondary mineral genesis from chlorite and serpentine in an ultramafic soil toposequence. *Soil Science Society of America Journal*, **67**, 1309–1317.
Lessovaia, S.N. and Polekhovsky, Y.S. (2009) Mineralogical composition of shallow soils on basic and ultrabasic rocks of eastern Fennoscandia and of the Ural Mountains, Russia. *Clays and Clay Minerals*, **57**, 476–485.
Lessovaia, S., Dultz, S., Polekhovsky, Y., Krupskaya, V., Vigasina, M., and Melchakova, L. (2012) Rock control of pedogenic clay mineral formation in a shallow soil from serpentinous dunite in the Polar Urals, Russia. *Applied Clay Science*, **64**, 4–11.
McGahan, D.G., Southard, R.J., and Claassen, V.P. (2008) Tectonic inclusions in serpentinite landscapes contribute plant nutrient calcium. *Soil Science Society of America Journal*, **72**, 838–847.
McGahan, D.G., Southard, R.J., and Claassen, V.P. (2009) Plant-available calcium varies widely in soils on serpentinite landscapes. *Soil Science Society of America Journal*, **73**, 2087–2095.
McKeague, J.A. and Day, J.H. (1966) Dithionite and oxalate extractable Fe and Al as aids in differentiating various classes of soils. *Canadian Journal of Soil Science*, **46**, 13–22.
McLean, E.O. (1982) Soil pH and lime requirement. Pp. 199–224 in: *Methods of Soil analysis*, *Part 2, Chemical and Microbiological Properties*, 2nd edition (A.L. Page, R.H. Miller, and D.R. Keeney, editors). Agronomy Monograph No. **9**. American Society of Agronomy and Soil Science Society of America, Madison, Wisconsin, USA.
Mehra, O.P. and Jackson, M.J. (1960) Iron oxides removed from soils and clays by a dithionite–citrate system buffered with sodium bicarbonate. *Clays and Clay Minerals*, **7**, 317–327.
Morrison, J.M., Goldhaber, M.B., Lee, L., Holloway, J.M., Wanty, R.B., Wolf, R.E., and Ranville, J.F. (2009) A regional-scale study of chromium and nickel in soils of northern California, USA. *Applied Geochemistry*, **24**, 1500–1511.
Nelson, D.W. and Sommers, L.E. (1982) Total carbon, OC, and organic matter. Pp. 539–557 in: *Methods of Soil Analysis, Part 2, Chemical and Microbiological Properties*, 2nd edition (A.L. Page, R.H. Miller, and D.R. Keeney, editors). Agronomy Monograph No. **9**. American Society of Agronomy and Soil Science Society of America, Madison, Wisconsin, USA.
Nkoumbou, C., Villieras, F., Barres, O., Bihannic, I., Pelletier, M., Razafitianamaharavo, A., Metang, V., Yonta Ngoune, C., Njopwouo, D., and Yvon, J. (2008) Physicochemical properties of talc ore from Pout-Kelle and Memel deposits (central Cameroon). *Clay Minerals*, **43**, 317–337.
Norrish, K. and Hutton, J.T. (1969) An accurate X-ray spectrographic method for the analysis of a wide range of geological samples. *Geochimica et Cosmochimica Acta*, **33**, 431–453.
O'Hanley, D.S. (1996) *Serpentinites: Records of Tectonic and Petrological History*. Oxford University Press, New York.
Oze, C., Bird, D.K., and Fendorf, S. (2007) Genesis of hexavalent chromium from natural sources in soil and groundwater. *Proceedings of the National Academy of Sciences*, **17**, 6544–6549.
Oze, C., Skinner, C., Schroth, A., and Coleman, R.G. (2008) Growing up green on serpentine soils: Biogeochemistry of serpentine vegetation in the Central Coast Range of California. *Applied Geochemistry*, **23**, 3391–3403.
Rabenhorst, M.C., Foss, J.E., and Fanning, D.S. (1982) Genesis of Maryland soils formed from serpentinite. *Soil Science Society of America Journal*, **46**, 607–616.
Rhoades, J.D. (1982) Cation exchangeable capacity. Pp. 149–157 in: *Methods of Soil Analysis, Part 2, Chemical and Microbiological Properties*, 2nd edition (A.L. Page, R.H. Miller, and D.R. Keeney, editors). Agronomy Monograph No. **9**. American Society of Agronomy and

https://doi.org/10.1346/CCMN.2015.0630204 Published online by Cambridge University Press

Soil Science Society of America, Madison, Wisconsin, USA.

Soil Survey Staff (1993) Examination and description of soils in the field. Pp. 59–196 in: *Soil Survey Manual*. Issued October, 1993. Handbook No. **18**, USDA-Soil Conservation Service, Washington, D.C.

Soil Survey Staff (2010) *Keys to Soil Taxonomy*, 12th edition. USDA, Natural Resources Conversation Services, Washington, D.C., 332 pp.

Suquet, H. (1989) Effects of dry grinding and leaching on the crystal structure of chrysotile. *Clays and Clay Minerals*, **37**, 439–445.

Wanze, M., Jagupilla, S.C., Moon, D.H., Christodoulatos, C., and Koutsospyros, A. (2008) Leaching mechanisms of Cr(VI) from chromite ore processing residue. *Journal of Environmental Quality*, **37**, 2125–2134.

Whittaker, R.H. (1954) The ecology of serpentine soils. IV. The vegetation response to serpentine soils. *Ecology*, **35**, 275–288.

Wicks, F.J. and O'Hanley, D.S. (1988) Serpentine minerals: structures and petrology. Pp. 91–167 in: *Hydrous Phyllosilicates (Exclusive of Micas)* (S.W. Bailey, editor). Reviews in Mineralogy and Geochemistry, **19**, Mineralogical Society of America, Washington, D.C.

Yongue-Fouateu, R., Yemefack, M., Wouatong, A.S.L., Ndjigui, P.D., and Bilong, P. (2009) Contrasted mineralogical composition of the laterite cover on serpentinites of Nkamouna-Kongo, southeast Cameroon. *Clay Minerals*, **44**, 221–237.

(*Received 5 May 2014; revised 8 April 2015; Ms. 873; AE: A. Thompson*)

https://doi.org/10.1346/CCMN.2015.0630204 Published online by Cambridge University Press